

See discussions, stats, and author profiles for this publication at: <https://www.researchgate.net/publication/45507554>

# Pulmonary vascular and cardiac effects of peroxynitrite decomposition in newborn rats

ARTICLE *in* FREE RADICAL BIOLOGY AND MEDICINE · NOVEMBER 2010

Impact Factor: 5.74 · DOI: 10.1016/j.freeradbiomed.2010.07.021 · Source: PubMed

CITATIONS

12

READS

32

12 AUTHORS, INCLUDING:



[Jaques Belik](#)

SickKids

61 PUBLICATIONS 1,140 CITATIONS

[SEE PROFILE](#)



[Crystal Kantores](#)

SickKids

29 PUBLICATIONS 497 CITATIONS

[SEE PROFILE](#)



[Julijana Ivanovska](#)

SickKids

16 PUBLICATIONS 122 CITATIONS

[SEE PROFILE](#)



[Peter H Backx](#)

University of Toronto

247 PUBLICATIONS 9,710 CITATIONS

[SEE PROFILE](#)



## Original Contribution

## Pulmonary vascular and cardiac effects of peroxynitrite decomposition in newborn rats

Jaques Belik<sup>a,b,c,\*</sup>, Danielle Stevens<sup>d</sup>, Jingyi Pan<sup>a</sup>, Brendan A.S. McIntyre<sup>a</sup>, Crystal Kantores<sup>e</sup>, Julijana Ivanovska<sup>e</sup>, Emily Z. Xu<sup>c</sup>, Christine Ibrahim<sup>e</sup>, Brian K. Panama<sup>c</sup>, Peter H. Backx<sup>c</sup>, Patrick J. McNamara<sup>a,b,c</sup>, Robert P. Jankov<sup>b,c,e</sup>

<sup>a</sup> Physiology and Experimental Medicine Program, The Hospital for Sick Children Research Institute, University of Toronto, Toronto, ON, Canada M5S 1A8

<sup>b</sup> Division of Neonatology, Department of Pediatrics, University of Toronto, Toronto, ON, Canada M5S 1A8

<sup>c</sup> Department of Physiology, University of Toronto, Toronto, ON, Canada M5S 1A8

<sup>d</sup> Maastricht University, 6202 Maastricht, The Netherlands

<sup>e</sup> Clinical Integrative Biology, Sunnybrook Research Institute, University of Toronto, Toronto, ON, Canada M5S 1A8

## ARTICLE INFO

## Article history:

Received 9 February 2010

Revised 25 June 2010

Accepted 26 July 2010

Available online 2 August 2010

## Keywords:

Neonate

Cardiomyocyte

Smooth muscle

Echocardiography

Nitrate

Free radicals

## ABSTRACT

Evidence implicates oxidative stress as playing a prominent role in the pathogenesis of pulmonary hypertension, to which peroxynitrite anion ( $\text{ONOO}^-$ ) may make a major contribution. Hypothesizing that removal of  $\text{ONOO}^-$  would attenuate chronic neonatal pulmonary hypertension, we examined the effects of a  $\text{ONOO}^-$  decomposition catalyst (FeTPPS) on pulmonary arteries in vitro, on primary cultured pulmonary artery smooth muscle cell (PASMC) and cardiomyocyte survival and growth, and on central hemodynamics in rat pups exposed to hypoxia (13%  $\text{O}_2$ ) for 7 days from birth. Daily FeTPPS (30 mg/kg ip) reduced lung nitrotyrosine content, attenuated vascular remodeling, and normalized pulmonary vascular resistance in hypoxia-exposed animals. FeTPPS attenuated proliferation and increased apoptosis of neonatal PASMCs in vitro. Isolated neonatal pulmonary arteries treated with FeTPPS showed reduced agonist-induced force development and enhanced endothelium-dependent and -independent relaxation, possibly via increased nitrate. However, we observed endothelial dysfunction, enhanced lung tissue phosphodiesterase 5 activity, and biventricular cardiac hypertrophy in air-exposed animals receiving FeTPPS. Further, in contrast to PASMCs, FeTPPS enhanced survival of newborn cardiomyocytes. We conclude that decomposition of  $\text{ONOO}^-$  with FeTPPS attenuates chronic hypoxia-induced pulmonary hypertension; however, it may negatively influence the modulation of normal pulmonary arterial relaxation function, cell survival, and growth.

© 2010 Elsevier Inc. All rights reserved.

Superoxide anion ( $\text{O}_2^{\bullet-}$ ) is a reactive oxygen species generated in increased amounts by the injured pulmonary vasculature and is believed to be involved in the pathogenesis of pulmonary arterial hypertension. A potentially major source of  $\text{O}_2^{\bullet-}$  is endothelial nitric oxide synthase (eNOS), which under normal conditions is primarily responsible for nitric oxide (NO) generation and vasomotor tone regulation in the pulmonary vasculature, but when “uncoupled”

generates  $\text{O}_2^{\bullet-}$  in addition to NO. Peroxynitrite anion ( $\text{ONOO}^-$ ) is a relatively stable product of the nearly diffusion-limited reaction between NO and  $\text{O}_2^{\bullet-}$ , which occurs almost 10 times faster than the reaction between superoxide dismutase (SOD) and  $\text{O}_2^{\bullet-}$  [1]. Chronic exposure of newborn rats to hypoxia (13%  $\text{O}_2$ ) from birth induces pulmonary  $\text{ONOO}^-$  generation as evidenced by increased nitrotyrosine formation in the lung [2]. Newborn lambs with severe pulmonary hypertension treated with intratracheal SOD had improved oxygenation and decreased lung oxidative stress [3]; both effects may have derived from decreased generation of  $\text{ONOO}^-$ .

We have previously shown that  $\text{ONOO}^-$  is a vasoconstrictor in newborn rat pulmonary arteries [4], in contrast to its dual vasoconstricting and vasodilatory effects on pulmonary vessels derived from adult animals [5,6]. At high concentrations,  $\text{ONOO}^-$  ( $10^{-4}$  M) reduced endothelium-dependent but not -independent vasorelaxation in vitro. The mechanism accounting for this apparent direct effect of  $\text{ONOO}^-$  on eNOS function is currently unclear, but others have shown that this molecule is capable of oxidizing the enzyme cofactor tetrahydrobiopterin to dihydrobiopterin, thus resulting in uncoupling

**Abbreviations:** AAT, aortic arterial acceleration time; FeTPPS, 5,10,15,20-tetrakis (4-sulfonatophenyl)porphyrinato iron(III); LVET, left ventricular ejection time; MWT, medial wall thickness;  $\text{ONOO}^-$ , peroxynitrite anion;  $\text{O}_2^{\bullet-}$ , superoxide anion; PAAT, pulmonary arterial acceleration time; PASMC, pulmonary artery smooth muscle cell; PDE 5, phosphodiesterase 5; PVR, pulmonary vascular resistance; VASP, vasodilator-associated phosphoprotein; RV/LV + S, right ventricular and left ventricular + septum; RVET, right ventricular ejection time; sGC, soluble guanylate cyclase; SVR, systemic vascular resistance.

\* Corresponding author. Physiology and Experimental Medicine Program, The Hospital for Sick Children Research Institute, University of Toronto, Toronto, ON, Canada M5S 1A8. Fax: +1 416 813 5245.

E-mail address: [Jaques.Belik@SickKids.ca](mailto:Jaques.Belik@SickKids.ca) (J. Belik).

and reduced NO generation. Finally, we found a temporal association (maximal at day 4) between immunoreactive nitrotyrosine on the walls of pulmonary resistance arteries and eNOS uncoupling in chronic hypoxia-exposed newborn rats [2], strongly suggesting that ONOO<sup>−</sup>-mediated eNOS uncoupling contributes to the pulmonary hypertension observed in these animals.

The goal of this study was therefore to evaluate the effect of a ONOO<sup>−</sup> decomposition catalyst, 5,10,15,20-tetrakis(4-sulfonatophenyl)porphyrinato iron(III) (FeTPPS) on structural and functional changes in chronic hypoxia-induced pulmonary hypertension in newborn rats. We hypothesized that ONOO<sup>−</sup> decomposition would reduce pulmonary arterial muscle contraction and enhance endothelium-dependent relaxation *in vitro*. We further hypothesized that daily FeTPPS administration would normalize pulmonary vascular resistance and attenuate the structural changes of chronic hypoxia-induced pulmonary hypertension.

## Experimental procedures

### Chemicals and reagents

Except where otherwise indicated, all chemicals and reagents were obtained from Sigma–Aldrich (Oakville, ON, Canada).

### Animal exposures and interventions

All procedures were conducted according to criteria established by the Canadian Council on Animal Care and were approved by the Animal Care Committees of the Sunnybrook and The Hospital for Sick Children Research Institutes. On their anticipated day of delivery, pathogen-free pregnant Sprague–Dawley dams (Taconic, Germantown, NY, USA) were placed in sealed 100×80×60-cm exposure Plexiglas chambers (BioSpherix, Redfield, NY, USA) with a 12/12-h light/dark cycle, with the temperature kept at 25±1 °C and humidity at 50%. Each litter, limited to 10–12 pups to control for nutritional effects, was nursed in either normoxia (21% O<sub>2</sub>) or hypoxia (13% O<sub>2</sub>) from birth until 7 days of life. The O<sub>2</sub> concentration, temperature, and humidity were continuously monitored, recorded, and regulated by computer using customized hardware (OxyCycler Model A84XOC; BioSpherix) and software (AnaWin2 Run-Time, 2.2.18; Watlow–Anafaze, St. Louis, MO, USA). Dams were exchanged daily between paired normoxia and hypoxia chambers to prevent any maternal toxicity and consequent nutritional effects on the pups. FeTPPS (30 mg/kg) in 0.9% saline vehicle or vehicle alone was administered *ip* (injected volume: 5 µl/g body wt) just before commencement of hypoxic exposure and daily thereafter. The dose of FeTPPS used was the same as that which has previously been reported to be effective in mice with ONOO<sup>−</sup>-mediated spinal cord injury [7]. At the end of each exposure period, pups were killed either by pentobarbital sodium overdose or by exsanguination after anesthesia.

### Preparation of tissue extracts

Tissue extracts were prepared in lysis buffer consisting of 50 mM Hepes (4-(2-hydroxyethyl)-1-piperazineethanesulfonic acid) buffered with sodium hydroxide to pH 7.4, 150 mM sodium chloride, 1% Triton X-100, 10% glycerol, 1.5 mM magnesium chloride, 2 mM EDTA, 1 mM phenylmethanesulfonyl fluoride, 2 µg/ml leupeptin, and 2 µg/ml pepstatin. Lung tissue was homogenized in a rotor/stator-type homogenizer, and pulmonary arteries and bronchi were frozen in liquid nitrogen and then ground with mortar and pestle before ice-cold lysis buffer was added. After 1 h on ice, the homogenates were centrifuged at 14,000 rpm for 20 min and the supernatant was collected and stored at −80 °C. Total protein concentration was measured using the Bradford method [8]; extracts were diluted to a final concentration of 4 mg/ml. Given the small size of pulmonary vessels, tissues were pooled such that each sample was derived from three animals.

### Organ bath studies

Third-generation lung intralobar pulmonary artery ring segments (average diameter 80–100 µm and length 2 mm) were dissected free and mounted in a wire myograph (Danish Myo Technology A/S, Aarhus, Denmark). Isometric changes were digitized and recorded online (Myodaq; Danish Myo Technology A/S). Tissues were bathed in Krebs–Henseleit buffer (NaCl, 115 mM; NaHCO<sub>3</sub>, 25 mM; NaHPO<sub>4</sub>, 1.38 mM; KCl, 2.51 mM; MgSO<sub>4</sub> · 7H<sub>2</sub>O, 2.46 mM; CaCl<sub>2</sub>, 1.91 mM; and dextrose, 5.56 mM) bubbled with air/6% CO<sub>2</sub> and kept at 37 °C. After 1 h of equilibration, the optimal tissue resting tension was determined by repeated stimulation with 128 mM KCl until maximum active tension was reached. All subsequent force measurements were obtained at optimal resting tension.

Pulmonary vascular muscle force generation was evaluated by stimulating with the thromboxane A<sub>2</sub> mimetic U46619. Contractile responses were normalized to the tissue cross-sectional area using the equation (width×diameter)×2 and expressed as mN/mm<sup>2</sup>. Relaxation was induced with the respective endothelium-dependent and -independent agonists acetylcholine and sodium nitroprusside, after precontraction with U46619 at concentrations equivalent to the EC<sub>75</sub>.

### Histological studies

Animals were anesthetized *ip* with ketamine (80 mg/kg) and xylazine (20 mg/kg). After the thoracic cavity was opened and the trachea cannulated, the pulmonary veins were divided. The pulmonary circulation was flushed with 1 ml PBS containing 1 U/ml heparin, via a needle inserted in the right ventricle, to clear the lungs of blood while the lungs were inflated at a constant pressure of 20 cm H<sub>2</sub>O. The lungs were then perfusion-fixed at 100 cm H<sub>2</sub>O pressure with ice-cold 4% (wt/vol) paraformaldehyde in PBS, excised *en bloc*, dehydrated, cleared in xylene, and embedded in paraffin. Sections (5 µm) were immunostained using an avidin–biotin–peroxidase method, as previously described in detail [1]. Slides were incubated with anti-nitrotyrosine rabbit polyclonal antiserum overnight at 4 °C at a dilution of 1/500 (2 µg/ml; Upstate Biotechnology, Lake Placid, NY, USA) followed by an anti-rabbit biotin-conjugated secondary antibody (Santa Cruz Biotechnology, Santa Cruz, CA, USA) for 1 h at room temperature. For assessment of percentage arterial medial wall thickness (%MWT), pulmonary arterioles were identified by the presence of both inner and outer elastic lamina using Weigert's resorcin–fuchsin (Rowley Biochemical, Danvers, MA, USA), digitally captured (Pixera Penguin 600CL; San Jose, CA, USA), and measured by an observer blinded to group identity, as previously described in detail [2]. Mean external diameter was calculated from measurements of round and ovoid vessels in two perpendicular planes (to account for any irregularities in vessel shape), excluding vessels that were cut tangentially (greater than threefold difference in MWT between perpendicular planes). Results are shown as mean values from three or four animals representing two litters per group.

### Measurement of PASMC proliferation and apoptosis

Primary culture PASMCs were obtained from Sprague–Dawley rats during the first week of life (generally days 2–4). After dissection and removal under sterile conditions, the third-generation intrapulmonary arterial tissue was cut into small pieces and incubated in Dulbecco's modified Eagle's medium (DMEM) containing papain (0.5 mg/ml), albumin (1 mg/ml), and dithiothreitol (1 mg/ml) on ice for 15 min and at 37 °C for a further 15 min and then centrifuged at 1200 rpm for 5 min. The pellet was resuspended in DMEM with 10% fetal bovine serum (FBS) and maintained in a humid incubator on air/5% CO<sub>2</sub> at 37 °C. The cells were passaged by trypsinizing with 0.25% trypsin–EDTA (GIBCO, ON, Canada) and used for experiments at passages 2–4. The specificity of the cultured cells was confirmed by

immunostaining with mouse monoclonal antibody raised against smooth muscle myosin heavy chain (SMMMS-1; Neomarkers) and smooth muscle calponin. PSMCs were treated with DMEM alone (control), DMEM with the apoptosis inducer paclitaxel (10  $\mu$ M; positive control for apoptosis), 10% (vol/vol) fetal bovine serum (positive control for proliferation), or varying doses of FeTPPS for 24 h at a gas phase of 21% O<sub>2</sub>, 5% CO<sub>2</sub>, and 74% N<sub>2</sub>. Proliferation was quantified using a WST-8 colorimetric assay kit (Cayman Chemical, Ann Arbor, MI, USA), according to the manufacturer's instructions. Apoptosis was quantified by measuring histone-complexed DNA fragments, using a commercially available colorimetric ELISA kit (Cell Death Detection ELISA<sup>PLUS</sup>; Roche, Laval, QC, Canada), according to the manufacturer's instructions. Values are expressed as a proliferation or apoptosis index, where the mean OD change in control cells was assigned a value of 1, and all other values were expressed as a multiple or fraction of the control value.

#### Estimation of cardiomyocyte survival

Primary rat neonatal cardiomyocytes were isolated and cultured from postnatal day 1 or 2 pups according to published protocols [9]. The cells were characterized by positive staining against mouse monoclonal cardiac  $\alpha$ -actin and the presence of beating colonies, clumps, and individual cells. Because of slow growth and the potential for overgrowth of contaminating myocardial fibroblasts when cultured for prolonged periods, insufficient cell numbers could be obtained for quantifying proliferation and apoptosis, as was performed for PSMCs. Instead, cardiomyocyte survival in the presence of varying doses of FeTPPS was examined using the Live/Dead Viability/Cytotoxicity kit for mammalian cells (Invitrogen, Carlsbad, CA, USA). The assay uses two-color fluorescence to differentially stain live and dead cells. The green calcein-AM is a general cellular stain for live cells, and the red ethidium homodimer-1 (EthD-1) intercalates into the DNA of dead and dying cells, specifically staining their nuclei. Cells were cultured for 2–3 days in DMEM with 1% FBS in the presence or absence of FeTPPS in 96-well black Optilux clear-bottom plates (BD Biosciences). On the day of the Live/Dead assay, cells were washed in 1 $\times$  HBSS and incubated in 4  $\mu$ M calcein-AM and 2  $\mu$ M EthD-1 for 20 min at 37 °C and visualized on a Nikon TE2000 inverted microscope equipped with an environmental chamber set to 37 °C.

To evaluate the peroxynitrite effect on cardiomyocyte apoptosis the following assay was conducted. The cardiomyocytes were plated in a 12-well dish at 200,000 cells per well and kept in DMEM/F-12 1/1 (vol/vol) containing 5% FBS for 48 h. For the apoptosis assay, cardiomyocytes were maintained in DMEM/F-12 (without FBS) in the absence (control) or presence of peroxynitrite (10<sup>−4</sup> M) for 24 h. The cells were subsequently trypsinized and resuspended in 100  $\mu$ l of binding buffer (140 mM NaCl, 2.5 mM CaCl<sub>2</sub>, 10 mM Hepes, pH 7.4). Next, 3.5  $\mu$ l of annexin V-FITC (Pharmingen, San Diego, CA, USA) and 3  $\mu$ l of propidium iodide were added and incubated for 15 min on ice. The myocytes were centrifuged (10,000 rpm for 20 s) and the pelleted myocytes were resuspended in 200  $\mu$ l of binding buffer and analyzed on a FACSCalibur flow cytometer (Becton–Dickinson, San Jose, CA, USA).

#### Nitrotyrosine ELISA

Nitrotyrosine, a “footprint” of ONOO<sup>−</sup>-mediated reactions, was measured in standards and total lung protein samples using a commercially available competitive ELISA kit (Cayman Chemical).

#### Western blot analysis of vasodilator-stimulated phosphoprotein (VASP) phosphorylation

Lung tissue was lysed in RIPA buffer containing protease and phosphatase inhibitors, fractionated by SDS–PAGE, transferred to polyvinylidene difluoride membranes, and blotted and band densities

were measured as previously described [3]. VASP phosphorylation, used as a marker of cGMP activity, was quantified by Phos-Tag acrylamide SDS–PAGE [4], according to a method previously reported in detail [5]. Membranes were blotted with anti-VASP (dilution 1:1000; Santa Cruz Biotechnology), yielding two bands, an upper band representing phosphorylated and a lower band representing unphosphorylated VASP (only one band was found when Phos-Tag was omitted from the resolving gel).

#### Phosphodiesterase (PDE) 5 activity assay

PDE 5 activity was assayed as previously described [6]. Briefly, lung tissue (approximately 100 mg per sample) was homogenized in lysis buffer supplemented with protease and phosphatase inhibitors. Samples were immediately placed on ice and assayed the same day. Protein was purified over a Centri-Spin 10 column to remove any phosphate contamination (Princeton Separations, Adelphia, NJ, USA), because the assay is dependent on free phosphate. Total protein was assayed for cGMP hydrolytic activity using a commercially available colorimetric cyclic nucleotide phosphodiesterase assay kit (Biomol, Plymouth Meeting, PA, USA) with or without MY-5445 (40  $\mu$ M), a PDE 5-specific inhibitor, to determine PDE 5-specific cGMP hydrolytic activity. Results are shown as PDE 5-specific picomoles of cGMP hydrolyzed per milligram of total protein per minute for each sample.

#### Cardiac ventricular weight

The right-to-left ventricular + septum weight ratio (RV/LV + S) was used as a surrogate marker for right ventricular hypertrophy resulting from pulmonary hypertension, as previously reported [10].

#### Echocardiography

Evaluation of PVR was performed on anesthetized animals spontaneously breathing room air, as previously described in detail [7]. Briefly, a short-axis view at the level of the aortic valve was obtained and the pulmonary artery was identified using color-flow Doppler. The pulmonary arterial acceleration time (PAAT) was measured as the time from the onset of systolic flow to peak pulmonary outflow velocity and the right ventricular ejection time (RVET) as the time from onset to completion of systolic pulmonary flow. A surrogate of PVR was calculated according to the formula 1/(PAAT/RVET). For measurements of systemic hemodynamics, a short-axis view at the level of the aortic valve was obtained and the aorta was identified using color-flow Doppler. The aortic arterial acceleration time (AAAT) and left ventricular ejection time (LVET) were then calculated from the aortic Doppler profile. AAAT was measured as the time from the onset of systolic flow to peak aortic outflow velocity and LVET was measured as the time from onset to completion of systolic aortic flow. A surrogate of systemic vascular resistance (SVR) was calculated according to the formula 1/(AAAT/LVET). Data from a canine model suggest that Doppler measurement of aortic blood flow velocity and acceleration can be used for the noninvasive assessment of changes in inotropy and afterload [11].

#### Data analysis

Data were evaluated by one- or two-way analysis of variance (ANOVA) with multiple comparisons obtained by the Tukey–Kramer test, or the unpaired Student *t* test when appropriate. Statistical significance was accepted at *P* < 0.05. All statistical analyses were performed with the Number Cruncher Statistical System (NCSS; Kaysville, UT, USA). Data are presented as means  $\pm$  SEM.

## Results

### Acute in vitro effects of FeTPPS on normal pulmonary arteries

Newborn pulmonary arterial muscle contraction in response to the thromboxane  $A_2$  analogue U46619 was significantly reduced in the presence of FeTPPS (Fig. 1A). The right-shifted force dose response in the presence of FeTPPS was also observed when the vessels were preincubated with the soluble guanylate cyclase (sGC) inhibitor ODQ, suggesting that the lower force in the FeTPPS-treated vessels was not sGC-mediated (Fig. 1B). Uric acid, an in vitro ONOO<sup>−</sup> scavenger [12], had effects similar to those of FeTPPS (Fig. 1C). Furthermore, no changes in dose response were observed when uric acid and FeTPPS were coadministered. Together, these findings are consistent with FeTPPS-induced changes in force being secondary to ONOO<sup>−</sup> decomposition (Fig. 1C).

To evaluate the effects of FeTPPS on vasorelaxation, precontracted (U46619; EC<sub>75</sub>) newborn pulmonary arteries were treated with acetylcholine (endothelium-dependent relaxation) or sodium nitroprusside (endothelium-independent relaxation). At the tested concentrations, FeTPPS induced a maximal twofold increase in the endothelium-dependent and -independent pulmonary arterial vasorelaxation responses (Fig. 2).

Decomposition of ONOO<sup>−</sup> by FeTPPS leads to a relative reduction in nitrite and increase in nitrate formation [13]. We therefore evaluated the newborn rat pulmonary arterial muscle tone response

to nitrite and nitrate in precontracted (U46619; EC<sub>75</sub>) pulmonary arteries. Nitrite ( $10^{-6}$  M) induced a  $10 \pm 4\%$  increase ( $P < 0.01$ ) in pulmonary arterial muscle contraction, whereas nitrate was associated with a maximum reduction in force at  $3 \times 10^{-7}$  M ( $14 \pm 1\%$ ;  $P < 0.01$ ). These findings are consistent with FeTPPS mediating arterial relaxation at least partly through increased generation of nitrate.

### Effects of FeTPPS on nitrotyrosine, arterial wall remodeling, cardiac ventricular weight, and pulmonary hemodynamics

The effects of daily FeTPPS administration on pulmonary arterial (Fig. 3A) and total lung (Fig. 3B) ONOO<sup>−</sup> content were evaluated by nitrotyrosine immunostaining and ELISA, respectively, in rat pups exposed from birth to either air or hypoxia. After 4 days of chronic hypoxia exposure immunoreactive nitrotyrosine in the pulmonary arterial wall was greatly increased by exposure to hypoxia, as previously reported [2]. This increase in nitrotyrosine was completely abrogated by treatment with FeTPPS (Fig. 3A). When total lung nitrotyrosine content was measured by ELISA, no increase in hypoxia-exposed animals was observed (Fig. 3B). However, treatment with FeTPPS greatly reduced nitrotyrosine in the lungs of both air- and hypoxia-exposed animals (Fig. 3B).

Effects of treatment with FeTPPS (30 mg/kg) on pulmonary vascular remodeling after 7 days of chronic hypoxia exposure (medial

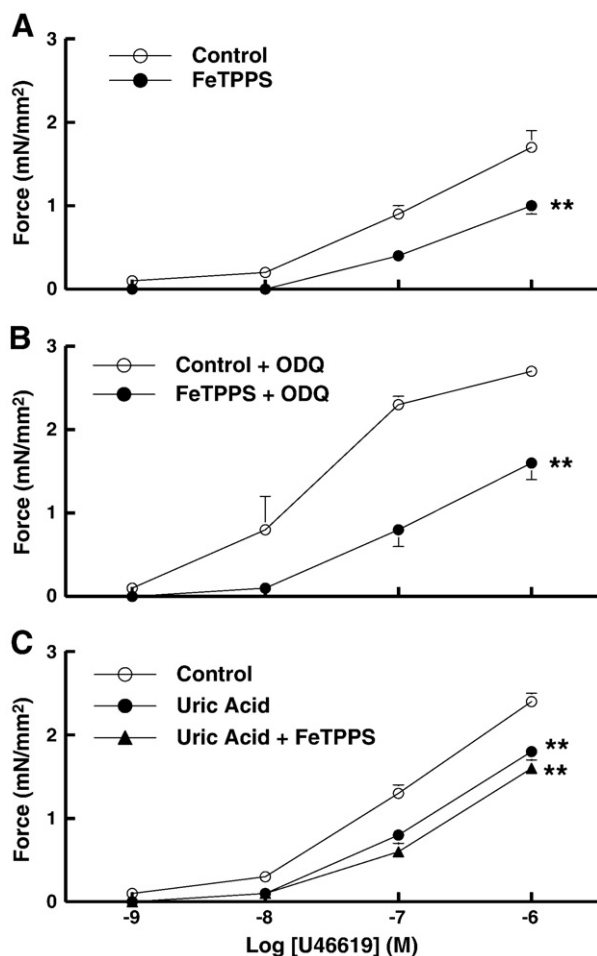


**Fig. 1.** Thromboxane  $A_2$  analogue (U46619)-induced force generation of pulmonary arteries obtained from newborn animals ( $N = 24$ ). Vessels were studied in the absence (control) or presence of (A) FeTPPS ( $10^{-4}$  M), (B) the soluble guanylate cyclase inhibitor ODQ ( $10^{-5}$  M), and (C) uric acid ( $5 \times 10^{-5}$  M).  $**P < 0.01$  compared with control values by two-way ANOVA and Tukey–Kramer multiple-comparison test.

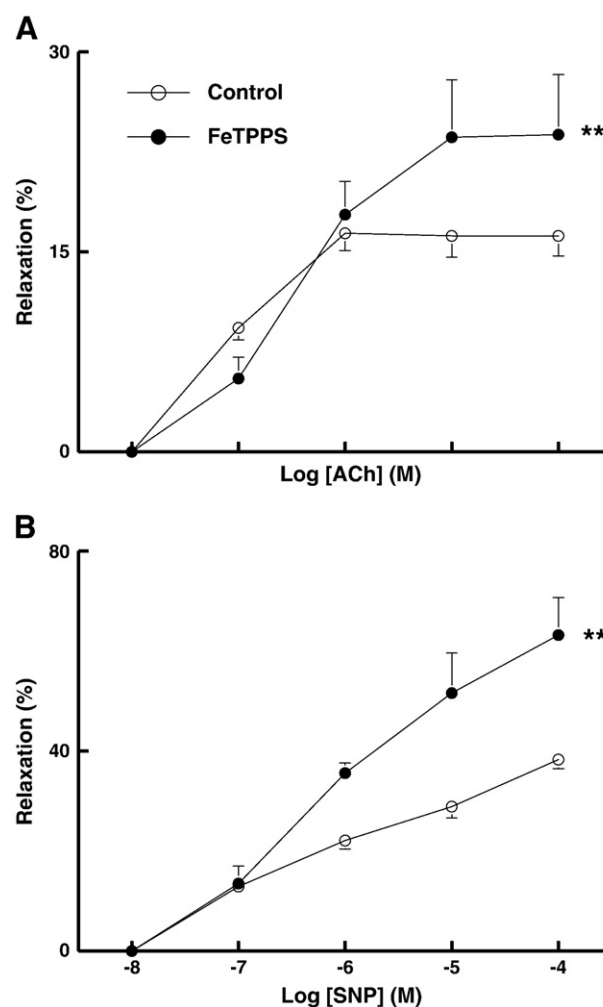


**Fig. 2.** (A) Endothelium-dependent (ACh—acetylcholine) and (B) -independent (SNP—sodium nitroprusside) relaxation response of U46619-precontracted (EC<sub>75</sub>) pulmonary arteries obtained from newborn rats ( $N = 25$ ). Vessels were studied in the absence (control) or presence of FeTPPS ( $10^{-4}$  M).  $**P < 0.01$  compared with control values by two-way ANOVA and Tukey–Kramer multiple-comparison test.



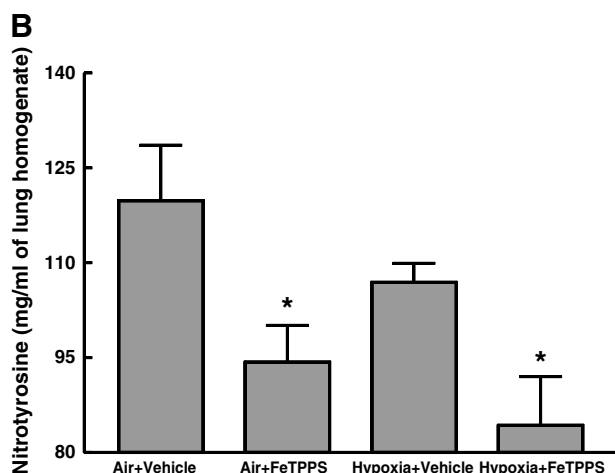
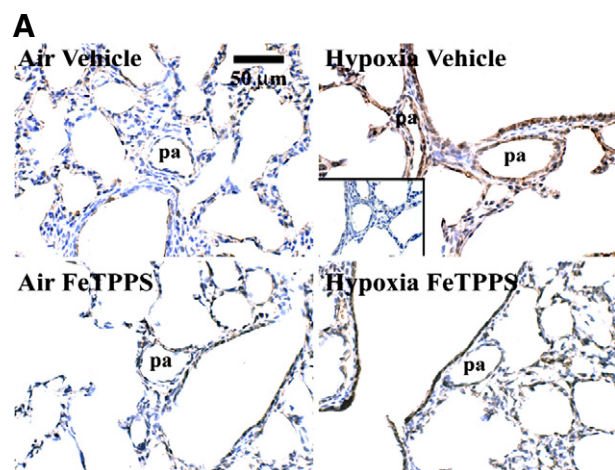


**Fig. 3.** (A) Representative lung immunostaining for nitrotyrosine in newborn animals exposed to air or 13% O<sub>2</sub> in the absence or presence of concomitant treatment with FeTPPS for 4 days (30 mg/kg/day). (B) Lung extract nitrotyrosine content measured by ELISA,  $N = 5$  lungs for each group. \* $P < 0.05$  compared with respective vehicle-treated animals by unpaired Student  $t$  test.

wall thickening and right ventricular hypertrophy) were evaluated. Compared with air-exposed newborn animals, %MWT in pulmonary resistance arteries and arterioles (10- to 60- $\mu$ m vessel diameter) was significantly increased ( $P < 0.01$ ) in the chronic hypoxia-exposed animals. Concurrent daily administration of FeTPPS to the pups significantly attenuated the hypoxia-induced increase in %MWT without affecting this parameter in air-exposed animals (Fig. 4). We measured the RV/LV + S ratio, as a marker of chronic pulmonary hypertension. This ratio was significantly increased ( $P < 0.01$ ) in the chronic hypoxia-exposed, compared with the air-exposed, pups (Fig. 5A). FeTPPS significantly reduced ( $P < 0.01$ ) the RV/LV + S values in the chronic hypoxia-treated animals.

Interestingly, we observed that the effects of FeTPPS treatment on cardiac ventricular weights were not limited to hypoxia-exposed animals. FeTPPS significantly increased ( $P < 0.01$ ) both right ventricular and left ventricular + septum weights, as well as total heart weight, in air-exposed animals (Figs. 5B, C, and D), with a proportionately greater effect on RV weight, leading to an increased RV/LV + S ratio. No significant change in the body weight was observed among the four groups of animals studied (Fig. 5E).

To evaluate whether FeTPPS-induced right ventricular hypertrophy was the result of an increase in PVR, we examined Doppler-derived indices of pulmonary arterial hemodynamics ( $N = 8$  per group). As expected, chronic exposure to hypoxia significantly increased the 1/(PAAT/RVET) and 1/(AAAT/LVET) ratios, as indirect

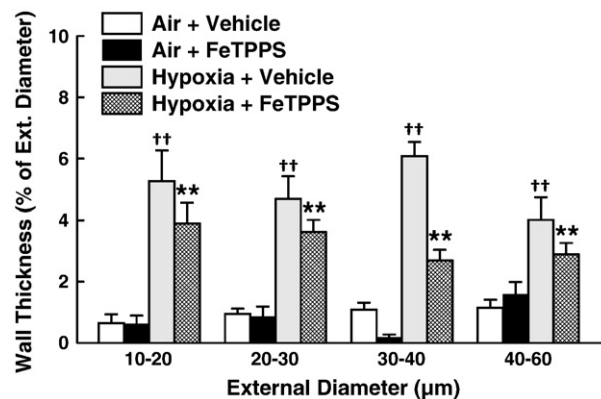


**Fig. 4.** Lung pulmonary arterial wall thickness as a percentage of external diameter in vessels from 10 to 60  $\mu$ m in diameter in air- and 13% O<sub>2</sub>-exposed animals in the absence or presence of concomitant treatment with FeTPPS for 4 days (30 mg/kg/day) in newborns. \*\* $P < 0.01$  compared with Hypoxia + vehicle group. †† $P < 0.01$  compared with air + vehicle group.  $N = 4$  animals per group. From every lung 8–46 vessels per diameter grouping shown on the horizontal axis were measured.

markers of increased PVR and SVR, respectively (Fig. 6). Treatment with FeTPPS significantly ( $P < 0.05$ ) attenuated raised PVR in chronic hypoxia-exposed animals, while having no effect in those exposed to air. We interpreted the latter observation as evidence that FeTPPS induced myocardial hypertrophy in air-exposed animals through modulatory effects on cardiomyocyte growth. The lack of FeTPPS effect on SVR supports this interpretation.

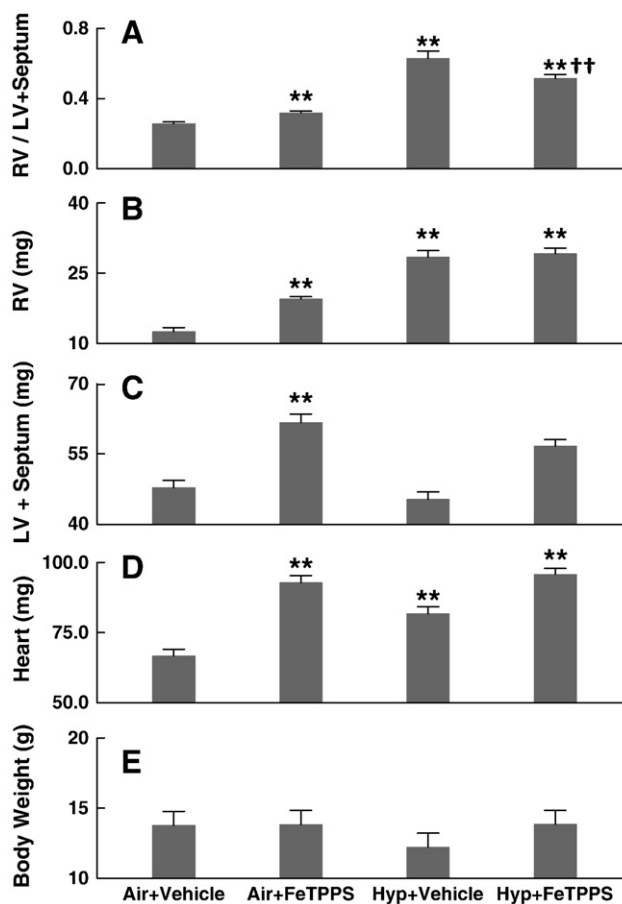


**Fig. 5.** (A) Right ventricular/left ventricular + septum ratio, (B) right ventricular weight, (C) left ventricular + septum weight, (D) total heart weight, and (E) body weight. \*\* $P < 0.01$  compared with air + vehicle group. Air + vehicle  $N = 19$ ; †† $P < 0.01$  compared with hypoxia + vehicle; air + FeTPPS  $N = 12$ ; hypoxia + vehicle  $N = 4$ ; hypoxia + FeTPPS  $N = 4$ .

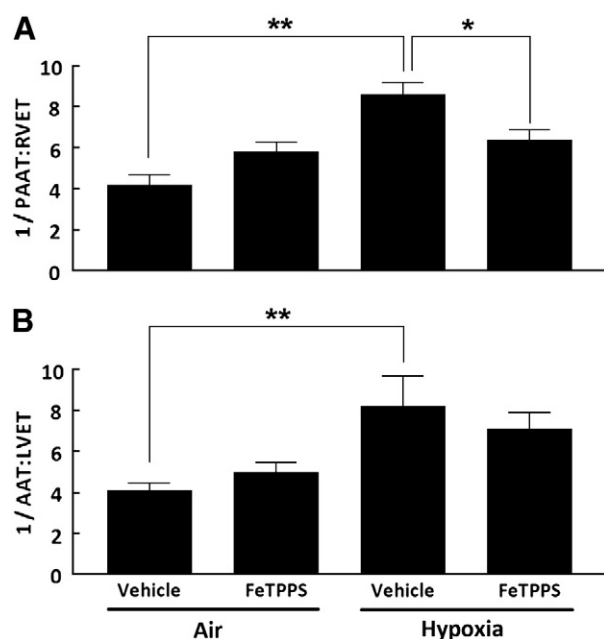


**Fig. 6.** Doppler-derived measurement of pulmonary vascular resistance in air- and hypoxia-exposed newborn rats treated with either vehicle or FeTPPS ( $N = 7$  or 8 pups per group). Pulmonary (PAAT) and aortic (AAAT) arterial acceleration times were measured as the time from the onset of systolic flow to peak outflow velocity and the right (RVET) and left (LVET) ventricular ejection times as the time from onset to completion of systolic pulmonary flow. Surrogates of pulmonary and systemic vascular resistance were calculated according to the formulas  $1/(PAAT/RVET)$  and  $1/(AAAT/LVET)$ , respectively. \*\* $P < 0.01$  and \* $P < 0.05$  by one-way ANOVA and Tukey–Kramer multiple comparisons.

#### Effects of FeTPPS on cell proliferation, apoptosis, and survival

Given the opposing effects of FeTPPS in reducing pulmonary arterial medial thickness, but increasing cardiac muscle weight, we evaluated the *in vitro* effect of FeTPPS on primary cultured PSMCs and cardiomyocytes derived from newborn rats. FeTPPS (100 nM) significantly increased PSMC apoptosis ( $P < 0.01$ ; Fig. 7A) while reducing serum-induced proliferation (Fig. 7B). In contrast, 24 h incubation with FeTPPS at  $10^4$  nM increased the survival of cardiomyocytes (Fig. 8), suggesting a mechanism by which FeTPPS may have led to cardiac ventricular hypertrophy.

We further evaluated the  $ONOO^-$  ( $10^{-4}$  M) effect on cardiomyocyte apoptosis.  $ONOO^-$  increased the annexin-V fluorescence intensity from  $5.8 \pm 0.5$  to  $15.0 \pm 3.2$  units ( $N = 3$ ;  $P < 0.05$ ). Given the low basal values it was not technically possible to quantify the FeTPPS-induced reduction in cardiomyocyte apoptosis rate, as qualitatively shown in Fig. 8.

#### Effects of treatment with FeTPPS on pulmonary arterial force contraction and relaxation

No differences in U46619-induced force dose response were observed, comparing air- and chronic hypoxia-exposed animals treated with either vehicle or FeTPPS (Fig. 9). Chronic exposure to hypoxia attenuated endothelium-dependent pulmonary arterial relaxation (Fig. 10A). Compared to vehicle-treated pups, chronic FeTPPS administration significantly attenuated endothelium-dependent vasorelaxation in air-exposed animals, but had no effect in animals exposed to hypoxia (Fig. 10A). Endothelium-independent pulmonary arterial vasorelaxation was unaltered either by exposure to hypoxia or by FeTPPS treatment (Fig. 10B).

To further explore a potential mechanism for reduced endothelium-dependent relaxation in response to FeTPPS, we evaluated markers of sGC-dependent cGMP production and function, given that impaired

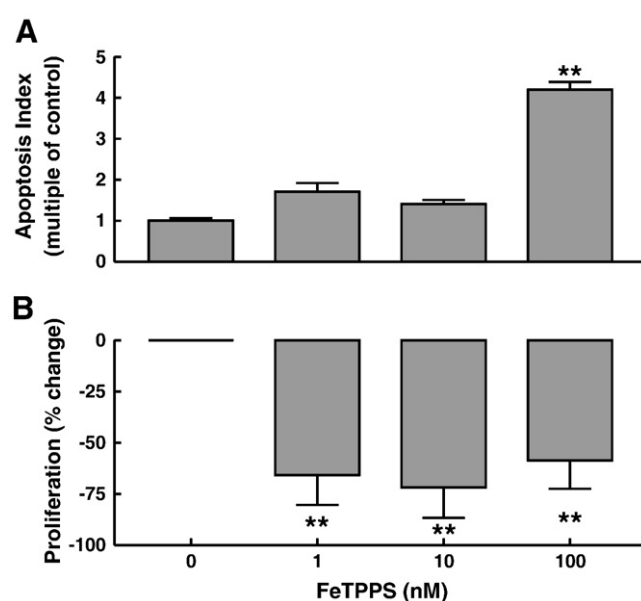


**Fig. 7.** Newborn primary pulmonary arterial smooth muscle cells (2nd–4th passage) were exposed to various *in vitro* concentrations of FeTPPS for 24 h. (A) Apoptosis index (multiple of control values). (B) Proliferation in response to fetal bovine serum stimulation. Values represent the FeTPPS-induced percentage decrease from serum-alone measurements. \*\* $P < 0.01$  compared with no-FeTPPS exposure values by one-way ANOVA and Tukey–Kramer multiple comparison test.  $N = 4$ –6 for each concentration of FeTPPS.

endothelium-dependent and -independent vasorelaxation has been documented in systemic vessels in association with increased  $ONOO^-$  production and reduced sGC expression [14]. We measured the lung activity of PDE 5 and the lung expression of phosphorylated VASP normalized to the nonphosphorylated protein, as a marker of cGMP activity. Treatment with FeTPPS led to a significant increase ( $P < 0.05$ ) in phosphodiesterase 5 activity in the air-exposed lung (Fig. 11A), suggesting that basal peroxynitrite production may limit activity of this enzyme. Increased PDE 5 activity with FeTPPS treatment was paralleled by decreased cGMP activity, as indicated by a significant decrease in p-VASP ( $P < 0.01$ ; Fig. 11B).

#### Discussion

When present in high concentrations,  $O_2^{\cdot-}$  may preferentially combine with NO to form the reactive nitrogen species  $ONOO^-$ , which has been linked to cellular injury and tissue inflammation [15].  $ONOO^-$  has been previously shown to induce pulmonary vasoconstriction in the newborn rat [4] as well as leading to airway and lung vascular remodeling [16,17]. As such,  $ONOO^-$  has been increasingly suspected as playing an important role in pulmonary vascular injury. Yet, to date, the effects of  $ONOO^-$  decomposition catalysts in experimental pulmonary hypertension have not been examined. In this study we evaluated the *in vitro* and *in vivo* effects of FeTPPS, a compound with well-described  $ONOO^-$  decomposition properties [13], on the normal and injured newborn rat lung.

We have previously reported that  $ONOO^-$  induces pulmonary arterial smooth muscle contraction in newborn rats and alters their vasorelaxation in response to endothelium-dependent and -independent agonists [2]. In this study, exposure of newborn pulmonary arteries to FeTPPS *in vitro* led to a significant decrease in agonist-stimulated force generation and improved relaxation, suggesting that  $ONOO^-$  is produced under basal conditions by the pulmonary vasculature.  $ONOO^-$  promotes nitrite formation, and its decomposition (with FeTPPS and other decomposition catalysts) results in nitrate generation in favor of nitrite. In this study, we showed that nitrate is a pulmonary arterial vasorelaxant agonist in the newborn rat, whereas nitrite led to vasoconstriction. Others have shown

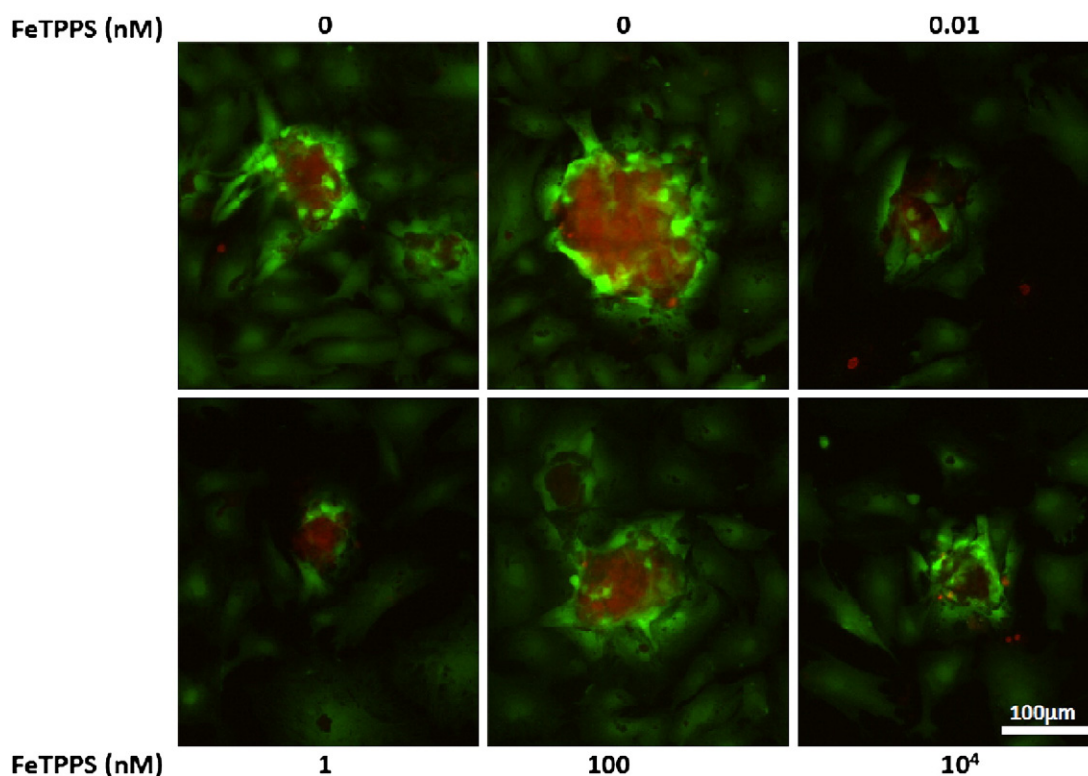


Fig. 8. Cellular viability of 1-day-old newborn rat cardiomyocyte beating colonies. Red EthD-1 intercalates into the DNA of dead and dying cells, specifically staining their nuclei.

that nitrate induces vasorelaxation independent of the endothelium and this effect is only partially related to its NO donor properties [13,18]. In the presence of ODQ ( $10^{-5}$  M), a compound known to effectively inhibit sGC activity in rat arteries [19,20], FeTPPS was still capable of reducing the pulmonary arterial force development in response to U46619. This finding strongly suggests that this ONOO<sup>-</sup> decomposition catalyst may act via direct nitrate-induced vasorelaxation rather than through stimulation of the NO–cGMP pathway.

Our findings in regard to the acute effects of FeTPPS *in vitro* conflict with the *in vivo* response after its chronic administration, suggesting that distinct pathways were altered by FeTPPS under the different experimental conditions. Our *in vitro* data are in keeping with a reduction in ONOO<sup>-</sup> content and increased nitrate generation contributing to vasorelaxation in response to FeTPPS. In contrast, chronic *in vivo* administration of FeTPPS to normal (air-exposed) animals led to attenuated endothelium-dependent relaxation and decreased p-VASP/VASP ratio, a surrogate marker for activity of the cGMP-dependent

kinase I [21,22], suggesting that sGC-dependent cGMP content was reduced, probably through increased PDE 5 activity. Although chronic FeTPPS treatment did not alter the pulmonary arterial endothelium-independent relaxation in this study, this does not necessarily contradict our finding that FeTPPS induced changes in PDE 5 activity. Because cGMP-independent mechanisms also contribute to NO-mediated vascular smooth muscle relaxation [23], such alternative pathways may offset the FeTPPS-induced upregulation of pulmonary arterial PDE 5 activity in FeTPPS-treated rats. We speculate, based on the

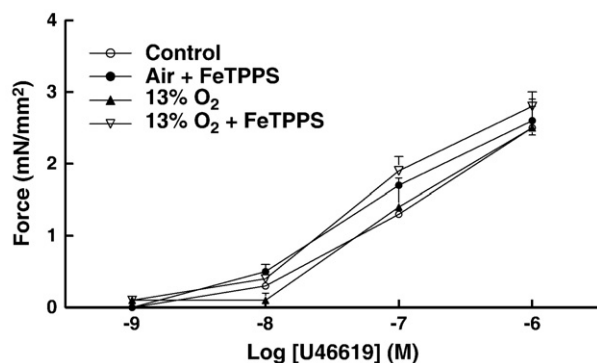


Fig. 9. U46619-induced force response in pulmonary arteries from 7-day air-exposed control and 13% O<sub>2</sub>-exposed animals with concurrent vehicle or FeTPPS (30 mg/kg ip daily) treatment. Air + vehicle N=13; air + FeTPPS N=12; hypoxia + vehicle N=10; hypoxia + FeTPPS N=6.

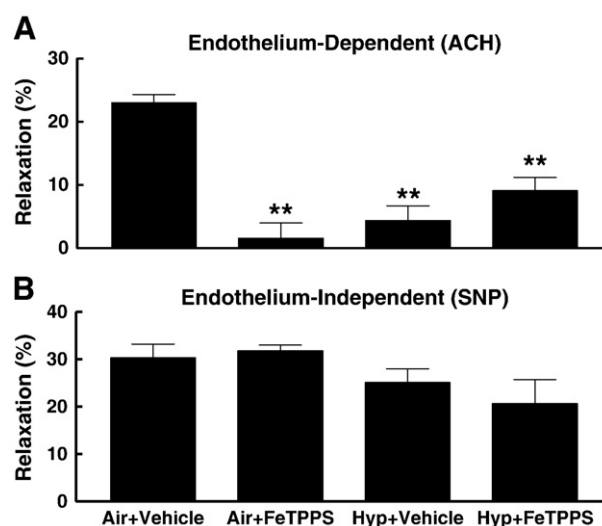
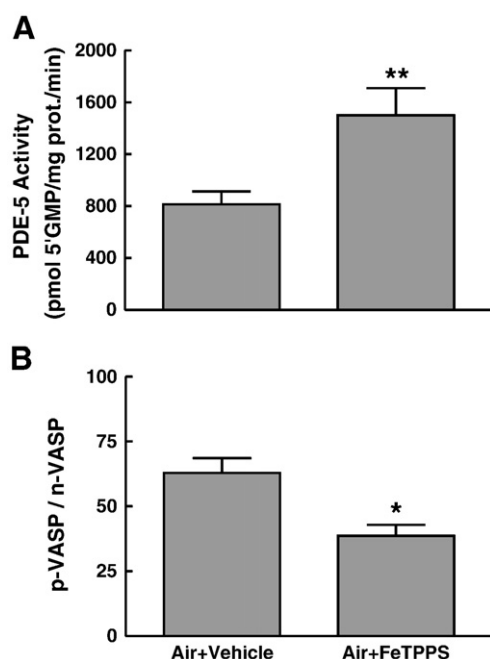


Fig. 10. (A) Endothelium-dependent (ACh—acetylcholine,  $10^{-4}$  M) and (B) -independent (SNP—sodium nitroprusside,  $10^{-4}$  M) pulmonary arteries from 7-day air-treated control and 13% O<sub>2</sub>-treated animals with concurrent FeTPPS (30 mg/kg ip daily or vehicle). Air + vehicle N=16; air + FeTPPS N=12; hypoxia + vehicle N=10; hypoxia + FeTPPS N=6. \*\* $P<0.01$  compared with air + vehicle values by one-way ANOVA and Tukey–Kramer multiple comparisons.





**Fig. 11.** (A) Seven-day vehicle (air + vehicle) and FeTPPS-treated (air + FeTPPS) newborn rat lung tissue extract PDE 5 activity. (B) Phosphorylated and nonphosphorylated vascular-associated phosphoprotein (p-VASP and n-VASP, respectively) ratio. \*\* $P < 0.01$  and \* $P < 0.05$  compared with air + vehicle values by unpaired Student *t* test.  $N = 4$  in each group.

above findings, that low physiological concentrations of  $\text{ONOO}^-$  (suppressed by FeTPPS) may be critical to normal endothelium-dependent pulmonary vascular relaxation.

We have previously reported that chronic exposure to hypoxia from birth leads to eNOS uncoupling and increased nitrotyrosine in the pulmonary vasculature during the first week of exposure [8]. Structural and functional changes in pulmonary hypertension in this model are evident by 7 days of life and are increasingly evident thereafter. In keeping with its known action as a  $\text{ONOO}^-$  decomposition catalyst, FeTPPS reduced lung nitrotyrosine content after 4 days of exposure to hypoxia. This was associated with a reduction in the magnitude of chronic hypoxia-induced vascular remodeling in small resistance pulmonary arteries by day 7 and in normalized pulmonary hemodynamics, as assessed by Doppler-derived indices of PVR. That the reduction in chronic hypoxia-induced pulmonary medial thickness in the newborn rats in this study was related to FeTPPS is further substantiated by its *in vitro* effect on PASMCs, whereby FeTPPS led to diminished proliferation and enhanced PASMC apoptosis in a concentration-dependent manner.

In contrast to our observations in pulmonary arterial smooth muscle, chronic administration of FeTPPS induced a significant increase in left and right ventricular mass, which was present even in air-exposed animals. The calculated SVR was not altered by chronic FeTPPS treatment in the air-exposed pups, suggesting that the observed left ventricular hypertrophy is not the result of an increased afterload.

Under normal conditions, tissue levels of  $\text{ONOO}^-$  are believed to be in the nano- to low micromolar range, suggesting a physiological role. Peroxynitrite has been shown by others to induce cardiomyocyte apoptosis, which is abrogated by FeTPPS [24], and this effect was confirmed in newborn rat myocytes in this study. When given *in vivo*, FeTPPS has been shown to have a cardioprotective effect by reversing endotoxemia-induced myocardial dysfunction in adult animals [25]. This study is the first, to our knowledge, to suggest that FeTPPS may enhance survival of cardiomyocytes and thus contribute to myocardial hypertrophy. Cardiomyocytes do not proliferate *in vitro*, preventing us from evaluating the FeTPPS and  $\text{ONOO}^-$  effects on

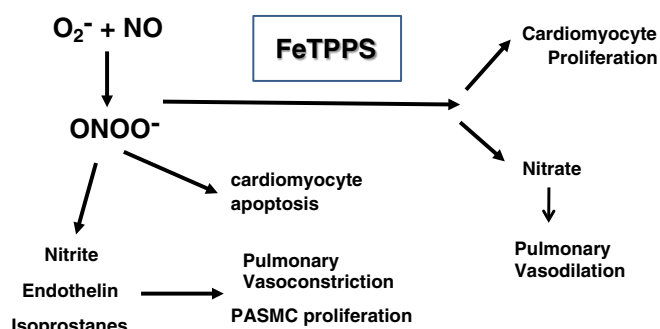


**Fig. 12.** Flow diagram depicting putative pathways of peroxynitrite and FeTPPS involvement in functional and structural changes in the newborn heart and pulmonary vasculature.

this process. Similarly, the low apoptosis rate of these cells under basal conditions prevented us from quantifying the FeTPPS-induced effect. Yet, taken together, our data strongly support the conclusion that the observed left and right ventricular hypertrophy documented in chronically FeTPPS-treated pups is secondary to a reduction in cardiomyocyte apoptosis.

Fig. 12 illustrates the various putative effects of  $\text{ONOO}^-$  and FeTPPS on the pulmonary circulation of the newborn.  $\text{ONOO}^-$  induces an increase in pulmonary arterial pressure and ultimately pulmonary hypertension via nitrite, endothelin, and isoprostane generation, as we have previously shown in newborn rats [4]. Under physiological conditions it has a protective effect on the heart, promoting cardiomyocyte apoptosis. Chronic exposure to a  $\text{ONOO}^-$  decomposition catalyst such as FeTPPS, although potentially beneficial to the pulmonary vasculature, promotes myocardial hypertrophy by inhibiting cardiomyocyte apoptosis.

In conclusion, although reducing physiological concentrations of  $\text{ONOO}^-$  decreases agonist-induced force and enhances pulmonary arterial vasorelaxation *in vitro*, its chronic administration to newborn rats attenuates normal vasorelaxation and induces cardiac ventricular muscle hypertrophy. These findings suggest that although  $\text{ONOO}^-$  may be critical to the pathogenesis of chronic hypoxia-induced pulmonary hypertension, the use of therapy aimed at its decomposition may have negative repercussions due to the potential physiological role of  $\text{ONOO}^-$  in modulating myocardial growth and endothelial function. The current findings add to concerns [2,26] about the limitations of strategies aimed at targeting reactive oxygen (or nitrogen) species in preventing neonatal disease.

## Acknowledgments

This work was supported by operating grants from the Canadian Institutes for Health Research, MOP 84290 (R.P. Jankov) and MOP 93710 (J. Belik), and an infrastructure grant from the Canada Foundation for Innovation (R.P. Jankov). Dr. Jankov is a CIHR New Investigator. Dr. Brian Panama is financially supported by a fellowship from the Heart and Stroke Foundation of Canada and the Richard Lewar Centre of Excellence. Drs. Belik and Backx are members of the Richard Lewar Centre of Excellence. Dr. Backx is a Career Investigator with the Heart & Stroke Foundation of Ontario.

## References

- O'Donnell, V. B.; Freeman, B. A. Interactions between nitric oxide and lipid oxidation pathways: implications for vascular disease. *Circ. Res.* **88**:12–21; 2001.
- Jankov, R. P.; Kantores, C.; Pan, J.; Belik, J. Contribution of xanthine oxidase-derived superoxide to chronic hypoxic pulmonary hypertension in neonatal rats. *Am. J. Physiol. Lung Cell. Mol. Physiol.* **294**:L233–L245; 2008.
- Lakshminrusimha, S.; Russell, J. A.; Wedgwood, S.; Gugino, S. F.; Kazzaz, J. A.; Davis, J. M., et al. Superoxide dismutase improves oxygenation and reduces

- oxidation in neonatal pulmonary hypertension. *Am. J. Respir. Crit. Care Med.* **174**: 1370–1377; 2006.
- [4] Belik, J.; Jankov, R. P.; Pan, J.; Tanswell, A. K. Peroxynitrite inhibits relaxation and induces pulmonary artery muscle contraction in the newborn rat. *Free Radic. Biol. Med.* **37**:1384–1392; 2004.
- [5] Ilesaki, T.; Gupta, S. A.; Kaminski, P. M.; Wolin, M. S. Inhibition of guanylate cyclase stimulation by NO and bovine arterial relaxation to peroxynitrite and H<sub>2</sub>O<sub>2</sub>. *Am. J. Physiol.* **277**:H978–H985; 1999.
- [6] Chabot, F.; Mitchell, J. A.; Quinlan, G. J.; Evans, T. W. Characterization of the vasodilator properties of peroxynitrite on rat pulmonary artery: role of poly (adenosine 5'-diphosphoribose) synthase. *Br. J. Pharmacol.* **121**:485–490; 1997.
- [7] Genovese, T.; Mazzon, E.; Esposito, E.; Muia, C.; Di, P. R.; Bramanti, P., et al. Beneficial effects of FeTSPP, a peroxynitrite decomposition catalyst, in a mouse model of spinal cord injury. *Free Radic. Biol. Med.* **43**:763–780; 2007.
- [8] Bradford, M. M. A rapid and sensitive method for the quantitation of microgram quantities of protein utilizing the principle of protein–dye binding. *Anal. Biochem.* **72**:248–254; 1976.
- [9] Wickenden, A. D.; Kaprielian, R.; Parker, T. G.; Jones, O. T.; Backx, P. H. Effects of development and thyroid hormone on K<sup>+</sup> currents and K<sup>+</sup> channel gene expression in rat ventricle. *J. Physiol.* **504** (Pt 2):271–286; 1997.
- [10] Le Cras, T. D.; Markham, N. E.; Tudor, R. M.; Voelkel, N. F.; Abman, S. H. Treatment of newborn rats with a VEGF receptor inhibitor causes pulmonary hypertension and abnormal lung structure. *Am. J. Physiol. Lung Cell. Mol. Physiol.* **283**:L555–L562; 2002.
- [11] Sohn, S.; Kim, H. S.; Han, J. J. Doppler flow velocity measurement to assess changes in inotropy and afterload: a study in healthy dogs. *Echocardiography* **19**:207–213; 2002.
- [12] Turan, N. N.; Yildiz, G.; Gumusel, B.; Demiryurek, A. T. Ischemic and peroxynitrite preconditioning effects in chronic hypoxic rat lung. *Exp. Lung Res.* **34**:325–341; 2008.
- [13] Misko, T. P.; Highkin, M. K.; Veenhuizen, A. W.; Manning, P. T.; Stern, M. K.; Currie, M. G., et al. Characterization of the cytoprotective action of peroxynitrite decomposition catalysts. *J. Biol. Chem.* **273**:15646–15653; 1998.
- [14] Kagota, S.; Tada, Y.; Nejime, N.; Nakamura, K.; Kunitomo, M.; Shinozuka, K. Chronic production of peroxynitrite in the vascular wall impairs vasorelaxation function in SHR/NDmcr-cp rats, an animal model of metabolic syndrome. *J. Pharmacol. Sci.* **109**:556–564; 2009.
- [15] Sugiura, H.; Liu, X.; Kobayashi, T.; Togo, S.; Ertl, R. F.; Kawasaki, S., et al. Reactive nitrogen species augment fibroblast-mediated collagen gel contraction, mediator production, and chemotaxis. *Am. J. Respir. Cell Mol. Biol.* **34**:592–599; 2006.
- [16] DeMarco, V. G.; Habibi, J.; Whaley-Connell, A. T.; Schneider, R. I.; Sowers, J. R.; Andresen, B. T., et al. Rosuvastatin ameliorates the development of pulmonary arterial hypertension in the transgenic (mRen2)27 rat. *Am. J. Physiol. Heart Circ. Physiol.* **297**:H1128–H1139; 2009.
- [17] Ichikawa, T.; Sugiura, H.; Koarai, A.; Yanagisawa, S.; Kanda, M.; Hayata, A., et al. Peroxynitrite augments fibroblast-mediated tissue remodeling via myofibroblast differentiation. *Am. J. Physiol. Lung Cell. Mol. Physiol.* **295**:L800–L808; 2008.
- [18] Kleschyov, A. L.; Oelze, M.; Daiber, A.; Huang, Y.; Mollnau, H.; Schulz, E., et al. Does nitric oxide mediate the vasodilator activity of nitroglycerin? *Circ. Res.* **93**: e104–e112; 2003.
- [19] Tseng, C. M.; Tabrizi-Fard, M. A.; Fung, H. L. Differential sensitivity among nitric oxide donors toward ODQ-mediated inhibition of vascular relaxation. *J. Pharmacol. Exp. Ther.* **292**:737–742; 2000.
- [20] Teixeira, C. E.; Priviero, F. B.; Todd Jr., J.; Webb, R. C. Vasorelaxing effect of BAY 41-2272 in rat basilar artery: involvement of cGMP-dependent and independent mechanisms. *Hypertension* **47**:596–602; 2006.
- [21] Mulsch, A.; Oelze, M.; Kloss, S.; Mollnau, H.; Topfer, A.; Smolenski, A., et al. Effects of in vivo nitroglycerin treatment on activity and expression of the guanylyl cyclase and cGMP-dependent protein kinase and their downstream target vasodilator-stimulated phosphoprotein in aorta. *Circulation* **103**:2188–2194; 2001.
- [22] Oelze, M.; Mollnau, H.; Hoffmann, N.; Warnholtz, A.; Bodenschatz, M.; Smolenski, A., et al. Vasodilator-stimulated phosphoprotein serine 239 phosphorylation as a sensitive monitor of defective nitric oxide/cGMP signaling and endothelial dysfunction. *Circ. Res.* **87**:999–1005; 2000.
- [23] Weisbrod, R. M.; Griswold, M. C.; Yaghoubi, M.; Komalavilas, P.; Lincoln, T. M.; Cohen, R. A. Evidence that additional mechanisms to cyclic GMP mediate the decrease in intracellular calcium and relaxation of rabbit aortic smooth muscle to nitric oxide. *Br. J. Pharmacol.* **125**:1695–1707; 1998.
- [24] Klassen, S. S.; Rabkin, S. W. The metalloporphyrin FeTPPS but not by cyclosporin A antagonizes the interaction of peroxynitrate and hydrogen peroxide on cardiomyocyte cell death. *Naunyn Schmiedeberg's Arch. Pharmacol.* **379**:149–161; 2009.
- [25] Lauzier, B.; Sicard, P.; Bouchot, O.; Delemasure, S.; Moreau, D.; Vergely, C., et al. A peroxynitrite decomposition catalyst: FeTPPS confers cardioprotection during reperfusion after cardioplegic arrest in a working isolated rat heart model. *Fundam. Clin. Pharmacol.* **21**:173–180; 2007.
- [26] Jankov, R. P.; Negus, A.; Tanswell, A. K. Antioxidants as therapy in the newborn: some words of caution. *Pediatr. Res.* **50**:681–687; 2001.